Eur. Phys. J. A **13**, 243–246 (2002)

THE EUROPEAN PHYSICAL JOURNAL A

In-beam Mössbauer study of ^{57}Fe using a secondary ^{57}Mn beam and ion implantation

Y. Kobayashi[1], Y. Yoshida[2], M.K. Kubo[3], Y. Yamada[4], A. Yoshida[1], H. Ogawa[1], H. Ueno[1], and K. Asahi[1]

[1] RIKEN, 2-1 Hirosawa, Wako-shi, Saitama 351-0198, Japan
[2] Shizuoka Institute of Science and Technology, Fukuroi, Shizuoka 437-8555, Japan
[3] Department of Chemistry, University of Tokyo, 7-3-1 Hongo, Bunkyo-ku, Tokyo 113-0033, Japan
[4] Department of Chemistry, Science University of Tokyo, Shinjuku, Tokyo 162-8601, Japan

Received: 1 May 2001 / Revised version: 31 August 2001

Abstract. We have succeeded in obtaining well-resolved Mössbauer spectra of ^{57}Fe arising from short-lived ^{57}Mn ($T_{1/2}$ = 1.45 min) in Si and $KMnO_4$. The Mössbauer spectra of ^{57}Fe in Si are well fitted with a curve consisting of two singlet lines, one being assigned as the *interstitial* Fe atoms and the other as *substitutional* ones. The relative intensities of the two lines infer that 60% of ^{57}Fe ($\leftarrow$ ^{57}Mn) atoms land at the *interstitial* sites and 40% at the *substitutional* sites at temperatures between 30 K and 296 K. The result for the $KMnO_4$ sample suggests a presence of an exotic chemical species corresponding to a higher valence state than Fe^{6+}.

PACS. 87.64.Pj Mössbauer spectroscopy – 23.90.+w Other topics in radioactive decay and in-beam spectroscopy (restricted to new topics in section 23) – 61.72.Ww Doping and impurity implantation in other materials – 31.30.Gs Hyperfine interactions and isotope effects, Jahn-Teller effect

1 Introduction

Emission Mössbauer spectroscopy offers unique information concerning the site occupation, dynamical behavior, and chemical states of extremely diluted atoms in a material. A large number of emission studies have been performed by the processes of chemical treatment or low-energy ion implantation for doping the radioactive Mössbauer probes into materials [1]. Recently, short-lived radioactive isotope beams (RI beams) at high energies, produced as secondary beams from the projectile fragmentation reaction, have been available at several laboratories in the world. The RI beams nowadays acquire an increasing importance in materials science: Their intensities are still considerably increasing; The implantation energies for the RI beams, extending up to a GeV region are by several orders of magnitude higher than those available in the conventional ion implantation techniques. Thus, RI beam particles can be applied not only as Mössbauer probes to obtain atomistic information on processes immediately after the implantation, but also as an effective tool to create exotic chemical species and/or valence states in materials.

The on-line Mössbauer technique using an energetic RI-beam provides a number of advantageous features over the conventional implantation Mössbauer method [2] and in-beam Mössbauer spectroscopy [3,4]. It is possible to implant Mössbauer probes into much deeper positions within straggling widths as narrow as a few μm. The time range for measurement can be selected by choosing probe nuclide of the appropriate half-life. In the case of ^{57}Mn, for instance, which decays to ^{57}Fe with a half-life of 1.45 min as shown in fig. 1, a Mössbauer measurement can be started about a few "minutes" after the implantation, while the in-beam Mössbauer experiment using Coulomb excitation and recoil implantation provides the time range of several hundred "nanoseconds" after implantation.

In the present studies, ^{57}Mn ions were implanted into samples of two different types, namely a semiconductor silicon and a chemical compound of potassium permanganate, $KMnO_4$. First of all, an Fe atom has been known to be one of the notorious impurities in a single crystal of Si. The on-line Mössbauer spectroscopy using an RI beam is considered to be one of the most powerful techniques to obtain atomistic information concerning the final lattice positions and dynamic behavior of Fe atoms in Si, because the concentration of the implanted nuclear probes is extremely low. Second, numbers of emission Mössbauer studies have been carried out to investigate ^{57}Fe species produced by EC decay of ^{57}Co, as a typical Mössbauer source, implanted into various matrices. However, there have been very rare applications of ^{57}Mn for chemistry because of its short half-life [5,6]. Mn occurs in various oxidation states in solids. Therefore, it is interesting to find out unusual valence states for ^{57}Fe arising from the ^{57}Mn decay, compared with those reached from ^{57}Co, in an appropriate matrix.

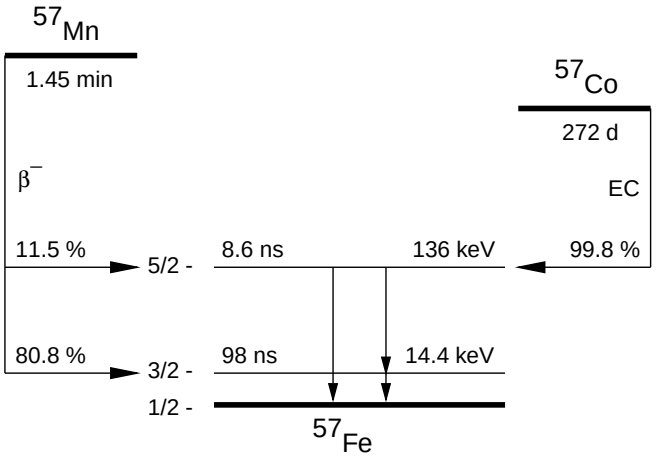

Fig. 1. Simplified level scheme of ^{57}Fe.

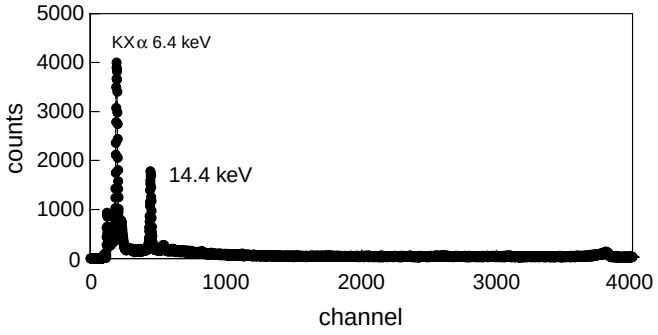

Fig. 2. Typical γ-ray spectrum of ^{57}Mn emitted from Si.

2 Experimentals

The secondary beam of ^{57}Mn was produced by a projectile fragmentation of a ^{59}Co primary beam impinging on a 1 mm thick Be production target. The energy and intensity of the primary beam were 80 MeV/nucleon and 250 enA (= 12 pnA), respectively. The ^{57}Mn beam was obtained through an in-flight isotope separation using RIPS (RIken Projectile-fragment Separator) at the Ring Cyclotron, RIKEN. The beam energy of ^{57}Mn was lowered before entering the stopper using an Al degrader of an appropriate thickness such that all the ^{57}Mn atoms were stopped in the sample. Two Si detectors, each placed in front of and behind the sample, were used together with a plastic scintillation counter mounted just before the sample chamber, in order to obtain the energy distribution of ^{57}Mn particles after the degrader through the time-of-flight (TOF) measurement. The implantation energy and typical intensity were finally evaluated to be about 17 MeV/nucleon and 2×10^5 particles/s, respectively.

The ^{57}Mn nuclei were implanted in two samples, a lightly B-doped FZ-silicon wafer and a pellet of $KMnO_4$, through a collimator having a ⌀30 mm opening. Each sample was mounted on an Al substrate holder and was cooled in a continuous liquid He-flow cryostat. The 14.4 keV γ-rays emitted from the sample were monitored by a CdZnTe detector during the Mössbauer measurement. Mössbauer spectra were collected by using two Parallel-Plate Avalanche Counters (PPAC) with an ^{57}Fe-enriched stainless-steel foil attached velocity transducers. The detailed view of the experimental layout used appears in refs. [7,8].

3 Results and discussion

3.1 Si

The typical γ-ray spectrum of the Si sample is shown in fig. 2. Both the γ peak at 14.4 keV and the KX_α-ray peak at 6.4 keV originating from ^{57}Fe were clearly observed with a rather low background. Mössbauer spectra for ^{57}Fe ($\leftarrow$ ^{57}Mn) in Si were measured at several temperatures between 30 and 296 K, as shown in fig. 3. The isomer shifts are given relative to iron metal at room temperature, and the sign of velocity follows the convention employed in the emission Mössbauer experiment. The whole spectrum could be fitted with two singlets, each corresponding to components A and B. The dominant component (component A) at 296 K, which has the isomer shift of 0.86(2) mm/s and an area intensity of 0.59, is assigned as an *interstitial* Fe atom in Si. The component B has the isomer shift of −0.05(4) mm/s, which is ascribed to a *substitutional* site in Si. The similar parameters of the components were observed in an in-beam experiment using Coulomb excitation and recoil implantation [9]. The

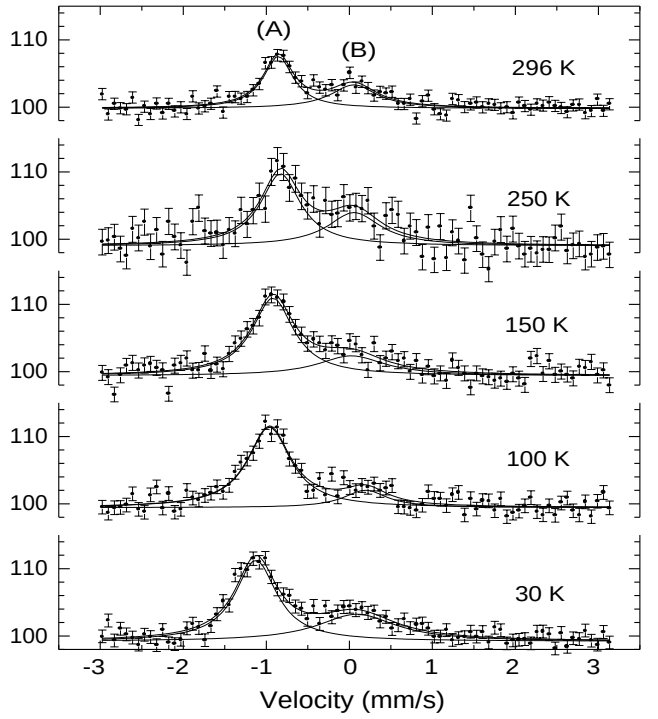

Fig. 3. Mössbauer spectra of ^{57}Fe ($\leftarrow$ ^{57}Mn) implanted into Si. The velocity scale is given relative to that in α-iron, and the convention for its sign is that employed in emission source experiment.

isomer shifts of both *interstitial* and *substitutional* lines are in good agreement with those obtained from theoretical calculations [2,10]. The ratio of area intensities did not change at any temperatures below 296 K. This means that 60% of ^{57}Fe ($\leftarrow$ ^{57}Mn) atoms end up at the *interstitial* sites, the remaining 40% being at the *substitutional* sites in Si. The line width of component B broadens with decreasing temperatures below 150 K. This may be explained by considering that the resonance lines tend to be a doublet at low temperatures due to the interaction with vacancies introduced by radiation. It is interesting to note that all the spectrum measured in the present study do not contain the doublet corresponding to an *amorphous* state ($\delta_{\mathrm{Fe}} = 0.23$ mm/s, $\Gamma = 0.74$ mm/s, and $E_Q = 0.83$ mm/s at 300 K) that has been observed in the previous study [2, 9]. It is suggested that the non-observation of the amorphous state may be attributed to differences in both the time scale for measurement after the implantation and defect structures around the probes.

Recently, G. Weyer *et al.* reported in-beam Mössbauer spectra for ^{57}Fe ($\leftarrow$ ^{57}Mn) in Si after the implantation at an energy of 60 keV at the on-line isotope mass separator ISOLDE at CERN [11]. Their results are somewhat different from those obtained in this study. It may be resulted from the much lower energy and much larger intensity (about 10^{11} ions/cm^2) of the implantation Mössbauer probes at ISOLDE as compared to those at RIKEN.

3.2 $KMnO_4$

So far the emission ^{57}Fe Mössbauer studies have been extensively carried out with doped and/or implanted ^{57}Co nuclide, but little attention has been paid to another mother nuclide ^{57}Mn. Mn sits next to Fe in the periodic table. However, the chemical properties of Mn are quite different from those of either Fe or Co. Mn occurs in various valence states from 0 up to 7+, and these states are known to be rather stable in ordinary solid-state chemistry. It is interesting to observe the valence states and the electron configuration of ^{57}Fe atoms arising from ^{57}Mn located at regular Mn sites in a molecule. Oxidation states synthesized in ^{57}Fe produced from the decay of ^{57}Mn might be different from those from the ^{57}Co decay. It is known that the after effects caused by the β decay around the decaying probes are not so important as compared to those caused by the EC decay. In the present study, $KMnO_4$ was used as a matrix to be irradiated by the ^{57}Mn nuclei. Mn ion in $KMnO_4$ is in a 7+ state and forms symmetric $[MnO_4]^-$ tetrahedron.

In-beam Mössbauer spectra of ^{57}Fe reached from the ^{57}Mn decay in $KMnO_4$ at temperatures 25 K and 155 K are shown in fig. 4 (top) and (bottom), respectively. Each spectrum was accumulated for over 20 hrs. The spectrum obtained at 25 K was tentatively analyzed in terms of two singlets, which are labeled as (A) and (B) in fig. 4. The isomer shifts for components A and B were derived to be 0.80 mm/s and -0.25 mm/s, respectively. The component A is assigned as the high-spin Fe^{2+} species from the value of the isomer shift.

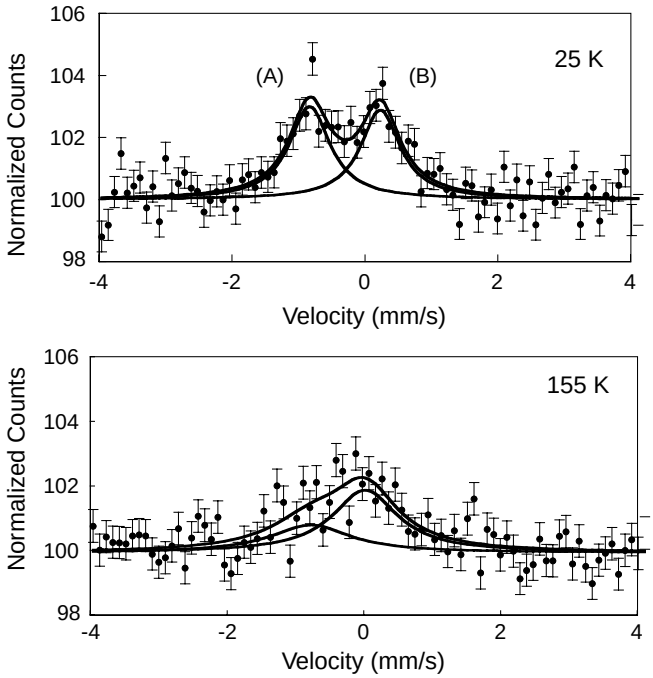

Fig. 4. Mössbauer spectra of ^{57}Fe ($\leftarrow$ ^{57}Mn) implanted into $KMnO_4$ at (top panel) 25 K and (bottom panel) 155 K. For the velocity scale and its sign convention, see caption to fig. 3.

In order to determine the chemical state for the component B, the correlation between the oxidation states and the isomer shifts for ^{57}Fe coordinated with octahedral and/or tetrahedral configurations of oxygen atoms were taken as reference [12,13]. The correlation is found extremely linear over whole range of oxidation states up to Fe^{6+}, of which the isomer shift reveals to be around -0.85 mm/s. However, for the higher oxidation states than Fe^{6+} in the $[FeO_4]^{n-}$ coordinations, the isomer shifts should deviate from the linear relation because of the increase in the covalency of tetrahedral Fe-O bonding. We carried out the molecular orbital calculation with DV-X_α method under an assumption that ^{57}Fe ($\leftarrow$ ^{57}Mn) ions substitute for the regular Mn ions in $KMnO_4$ and that the ^{57}Fe form the $[FeO_4]^{n-}$ tetrahedron with a distance similar to that in the Mn-O bond. The results yielded that the total electron population in the $3d$ orbitals of Fe atom decreased with a decrease of the number of electrons in the antibonding orbitals in a region between $3d^6$ (Fe^{2+}) and $3d^2$ (Fe^{6+}) configurations, but that in higher valence states up to Fe^{8+} the $3d$ population increased relatively because the covalency rose to predominate. Since the strong covalency leads to a contribution of the $4s$-electrons to the chemical bonding, the absolute value of the isomer shift should decrease. It suggests that the component B corresponds to be in a higher valence state with a strong covalency than Fe^{6+}.

The spectrum at 155 K, although a sufficient statistics was not reached, could be fitted with two components in the same manner as that at 25 K. Both resonance lines became broader than the result at 25 K. It is suggested that this phenomenon resulted from a certain dynamical effect

of implanted atoms. Furthermore, to discuss the site occupancies for ^{57}Fe ions, detailed temperature-dependence experiments and calculation by SCF-X_α and Gaussian98 procedures are being performed.

4 Conclusion

The on-line ^{57}Fe Mössbauer spectroscopic study combined with the ion implantation using a secondary ^{57}Mn beam has been performed for two different types of samples, Si and $KMnO_4$. The Mössbauer spectra of ^{57}Fe in Si have been well fitted with two singlet lines assigned, respectively, as the *interstitial* and the *substitutional* Fe atoms. The final site distribution of ^{57}Fe ($\leftarrow$ ^{57}Mn) in Si has been determined from the observed intensity ratio between the two lines: 60% of Fe atoms end up at the *interstitial* sites while the remaining 40% are located at the *substitutional* sites in the temperature range from 30 and 296 K. On the other hand, the implantation experiment of ^{57}Mn into $KMnO_4$ suggests a possible occurrence of an exotic chemical species corresponding to a higher valence state than Fe^{6+}. The present in-beam technique can be extended to a wide variety of Mössbauer probes and, therefore, will provide new applications for materials science research complementary to synchrotron experiments.

References

1. H. de Waard, L. Niesen, *Mössbauer Spectroscopy Applied to Inorganic Chemistry* (Plenum, New York, 1987) p. 1.
2. G. Langouche, Hyperfine Interact. **72**, 217 (1992).
3. R. Sielemann, Y. Yoshida, Hyperfine Interact. **68**, 119 (1991).
4. Y. Yoshida, Hyperfine Interact. **113**, 183 (1998).
5. R.S. Preston, B.J. Zabransky, Phys. Lett. A **55**, 179 (1975).
6. M. Nakada *et al.*, Bull. Chem. Soc. Jpn. **65**, 1 (1992).
7. Y. Kobayashi *et al.*, Hyperfine Interact. C **3**, 273 (1998).
8. Y. Kobayashi *et al.*, Hyperfine Interact. **126**, 417 (2000).
9. P. Schwalbach *et al.*, Phys. Rev. Lett. **64**, 1274 (1990).
10. J. Kübler *et al.*, Z. Phys. B **92**, 155 (1993).
11. G. Weyer *et al.*, Physica B **273-274**, 363 (1999).
12. N.S. Kopelov, *Mössbauer Spectroscopy of Sophisticated Oxides* (Akademiai Kiado, Budapest, 1997) p. 329.
13. F. Menil, J. Phys. Chem. Solids **46**, 763 (1985).